J Mol Model (2013) 19:3683–3694
DOI 10.1007/s00894-013-1905-x

ORIGINAL PAPER

# Synthetic and quantum chemical study on the regioselective addition of amines to methyl maleamate

**Ákos Rácz · András Váradi · Károly Mazák · József Kökösi · Béla Noszál**

Received: 30 January 2013 / Accepted: 30 May 2013 / Published online: 19 June 2013


**Abstract** Synthetic and theoretical studies were performed to gain insight into the regioselectivity in the mechanism of aspartyl-isoaspartyl formation, modeled by additions of ammonia and primary amines to methyl maleamate. Reactions between maleamate and aliphatic, araliphatic amines or O-methyl acetimidate lead to the formation of N-substituted isoasparaginates. The size of the amine and the activating effect of the amide and ester group on the double bond are the determining factors of the site of addition. The formation of both isomers was observed only in the case of ammonia addition. The regioselectivity was predicted on the basis of the charge distribution for low-energy methyl maleamate conformers, calculated at the B3LYP/6-311++G(2df,2pd)//B3LYP/6-31+G(d) level, both in gas phase and in methanol. The methyl isoasparaginate over methyl asparaginate product ratio was computed based on the free energy Boltzmann distribution of their conformers. The calculated 2 : 1 ratio is in agreement with the experimental regioselectivity of the addition of nitrogen nucleophiles.

**Keywords** aza-Michael addition · Methyl maleamate · N-nucleophiles · Regioselectivity · IEF-PCM/B3LYP calculations

## Introduction

Post-translation modifications of endogenous protein side chains have the ability to influence structure and biological activity [1, 2]. The historically unresolved problem of aspartyl peptide bond rearrangements leading to β-peptide formation is the focus of numerous biological, biochemical and chemical studies [3–5]. Aspartates and asparagines can undergo intramolecular cyclization to form a five-member succinimide ring through the nucleophilic attack of the adjacent peptide bond amide nitrogen on the side-chain carbonyl [2, 6]. Succinimides are unstable and undergo rapid hydrolysis to a mixture of aspartate and isoaspartate products (Fig. 1). The rearranged beta-peptide residue can affect both the structure and function of polypeptides and may underlie a portion of the aging-related loss of cellular and tissue function [7, 8]. The physiological importance of isoaspartate formation is supported by the presence of the highly conserved enzyme protein isoaspartate methyltransferase (PIMT), which catalyzes transfer of a methyl group from S-adenosylmethionine to the α-carboxyl group of an isoaspartate to stimulate reformation of the succinimide [9]. Subsequent hydrolysis of this ring results in a fraction of the original isoaspartates being converted to aspartates. Isoaspartates remain the predominant product (65–85 %) of succinimide hydrolysis, multiple rounds of repair are required for more complete conversion of an isoaspartate to aspartate. This represents true repair only when the initiating residue was an aspartate as asparagines are not regenerated [10].

Other biochemical transformations are also known for reversible carbon–nitrogen bond breaking leading to modified structures of amino acids. Aspartate ammonia lyases

**Electronic supplementary material** The online version of this article (doi:10.1007/s00894-013-1905-x) contains supplementary material, which is available to authorized users.

Á. Rácz (✉) · A. Váradi · K. Mazák · J. Kökösi · B. Noszál
Department of Pharmaceutical Chemistry, Semmelweis University, Hőgyes E. u. 9., 1092 Budapest, Hungary
e-mail: racz.akos@pharma.semmelweis-univ.hu

A. Váradi
e-mail: varadi.andras@pharma.semmelweis-univ.hu

K. Mazák
e-mail: mazak.karoly@pharma.semmelweis-univ.hu

J. Kökösi
e-mail: kokosi.jozsef@pharma.semmelweis-univ.hu

B. Noszál
e-mail: noszal.bela@pharma.semmelweis-univ.hu

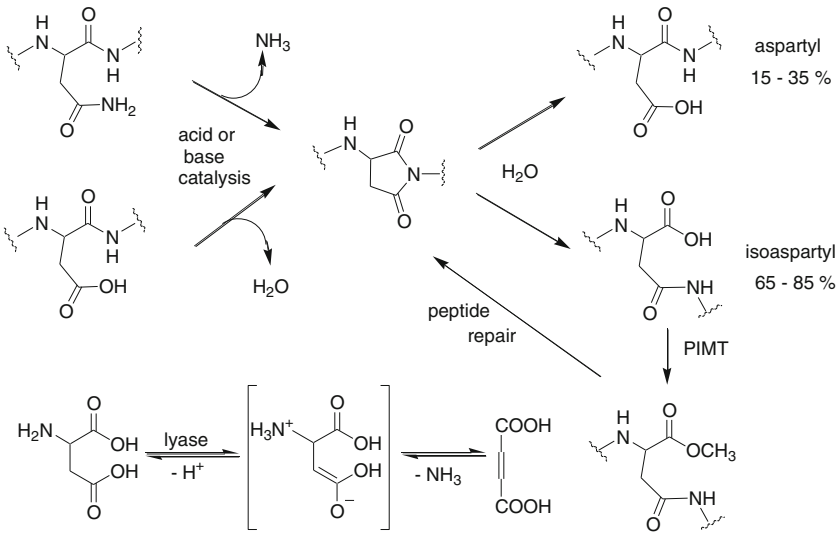


**Fig. 1** Interconversion of L-asparaginyl, L-isoaspartyl and L-aspartyl residues

catalyze the reversible elimination of ammonia from L-aspartate to yield fumarate [11] (Fig. 1). The reverse reaction, i.e., the amination of fumarate, is also catalyzed by different aspartate ammonia lyases [12]. The yields are usually quantitative, and the product L-aspartic acid is obtained in over 99 % enantiomeric purity. The industrial production of aspartame is based on this reaction [13]. In spite of the well-known biochemical significance of fumarate/maleamate, no comprehensive report on the interaction between these two pathways has ever appeared.

Maleate and its amide, maleamate are inhibitors of enzymes in cellular metabolism of aspartate [14]. Their reactivities, including Michael-acceptor properties are fundamental factors to elucidating their biological roles, in relation with post-translational peptide modifications. Under physiological conditions maleate is transformed by nucleophilic addition (OH, R-$NH_2$, SH) to malate, aspartate or thiosuccinate derivatives.

The endogenous maleamate formation (maleamate pathway) was observed during oxidative metabolism of pyridine compounds (NAD, NADH) [15, 16], and maleamate is an intermediate in the catabolism of gentisate [17]. The cyclic elimination mechanism of amides may lead to a maleamate product (Fig. 2) [18].

We have recently reported the selective synthesis [19] and physicochemical investigation [20] of NMDA and its amide derivatives by the Michael addition of methylamine to unsymmetrical maleamic and fumaric acid esters. The reaction could be controlled effectively and both regioisomers could be prepared with good-to-high selectivity. We also realized the importance of aspartyl-rearrangement [21], which prompted us to elucidate the influencing factors of regioselective aspartate formation related to endogenous peptide recovery.

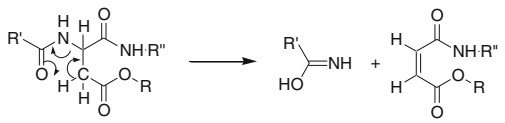

**Fig. 2** Cyclic elimination mechanism of amides leading to maleamate

## Materials and methods

### Experimental

All reagents and solvents were purchased from Sigma-Aldrich (St. Louis, MO), and were used as received. Melting points were taken on a Boethius apparatus and are uncorrected. Elemental analyses (C, H, N) were carried out on a Carlo Erba NA-1500 analyzer (http://www.carloerbareagents.com/), the results were within 0.4 % of the theoretical values. Mass spectra were recorded with a Thermo Finnigan LCQ Advantage LC-MS spectrometer (http://www.thermoscientific.com), used in ESI positive or negative ion mode. NMR spectra were recorded on a 600 MHz Varian VNMRS instrument (http://www.agilent.com). DMSO-$d_6$ (TMS as internal standard) was used as solvent.

The $^{1}$H- and $^{13}$C-NMR spectra of the compounds were assigned based on one and two-dimensional, homo- and hetero-nuclear NMR experiments. The product ratio (Table 1) was determined by integration of the methine proton signals in the NMR spectra of the crude isomer mixtures.

### *General procedure for N-alkyl-DL-isoasparagine β-methyl esters*

To a methanolic solution (8 ml) of methyl maleamate (0.01 mol), methanol solution (4 ml) of amine (0.01 mol) was added at 0 °C. The reaction mixture was stirred for 24 h at 20 °C. The solvent was evaporated in vacuo to dryness. A transparent oil of N-alkyl-DL-isoasparagine β-methyl esters was obtained in good yield. (Table 1)

The isoasparagine β-methyl ester and its other N-substituted derivatives were prepared in a similar manner by using ammonia

**Table 1** 1,4-Addition products of amines to methyl maleamate

| | R | Yield | Melting point (°C) | Ratio of i/a | Ratio of i/a NaOMe/MeOH | CH i (ppm) | CH a (ppm) |
|---|---|---|---|---|---|---|---|
| 1 | H | 66 | – | 72:28 | 30:70 | 3.34 | 3.28 |
| 2 | $CH_3$ | 98 | – | 100 | 26:74 | 3.29 | 3.18 |
| 3 | $C_2H_5$ | 95 | – | 100 | 23:77 | 3.28 | 3.21 |
| 4 | $C_3H_7$ | 91 | – | 100 | 21:79 | 3.39 | 3.26 |
| 5 | n-$C_4H_9$ | 84 | – | 100 | 21:79 | 3.35 | 3.32 |
| 6 | Cyclohexyl | 76 | 41–44 | 100 | 19:81 | 3.36 | 3.30 |
| 7 | $C_6H_5$-$CH_2$- | 96 | 112–114 | 100 | 22:78 | 3.72 | 3.57 |
| 8 | $C_6H_5$-$CH_2$-$CH_2$- | 87 | 77–78 | 100 | 24:76 | 3.42 | 3.35 |
| 9 | 2-(Imidazol-4-yl) -ethyl | 92 | 53–54 | 100 | 17:83 | 3.46 | 3.32 |
| 10 | $C_6H_5$ | 89 | 90–93 | 100 | 20:80 | 3.84 | 3.68 |
| 11 | 2-Pyridyl | 74 | 126–127 | 100 | 15:85 | 3.97 | 3.83 |

or the appropriate amine in methanolic solution. Analytically pure samples were isolated by a modified procedure: the crude product was dissolved in ethyl acetate and washed with 2 % aq. acetic acid, and then 5 % aq. sodium carbonate solution, dried over anhydrous magnesium sulfate and the solvent was evaporated under reduced pressure. In the case of aromatic amines the ethyl acetate solution was decolorized by charcoal. (Table 1) Spectroscopic details and elemental analyses are given in Supplementary material.

*O-methoxyethylidene-DL-isoasparagine β-methyl ester (**12**)*

Methyl acetimidate hydrochloride salt (1,09 g) was dissolved in methanol (20 mL) and cooled to 0 °C. 0.23 g sodium was dissolved in metanol (5 mL) and added drop-wise to imidate salt solution. After stirring the reaction mixture at 0 °C for 30 min the precipitated sodium chloride was filtered and methyl maleamate (1.29 g, 0.01 mol) was added to the solution. The reaction mixture was stirred for 24 h at 20 °C. The solvent was evaporated in vacuo to dryness. The residue was taken up in ethyl acetate (30 mL), extracted with 5 % sodium carbonate solution (2×10 mL and brine (2×10 mL. The solution was dried over sodium sulfate and evaporated in vacuo to give a colorless oil of 12 (1.09 g, 54 %).

$^1$H-NMR (DMSO-d6, 600 MHz): δ=2.03 (3H,s), 3.08 (2H, d, *J*=6.48), 3.58 (3H,s), 3.73 (3H,s), 4.54 (1H, t, *J*=6.48). $^{13}$C-NMR: 34.5 (3-CH2), 37.1 (N-Me), 48.6 (OMe), 64.8 (2-CH), 172.70 (C=N),173.3 (4-C=O) 176.2 (1-C=O). MW = 202,21 ESI-MS m/z: 202.28 M + H]$^+$ Anal. Calc. for $C_8H_{14}N_2O_4$ C = 47.52 % H = 6.98 %, *N*=13.85 %,

Found C = 47.59 %, H = 7.01 %, *N*=13.73 %

*N-acetyl-DL-isoasparagine β-methyl ester (**13**)*

O-methoxyethylidene-DL-isoasparagine β-methyl ester (**12**) (1 g, 0.05 mol) was dissolved in 5 % acetic acid solution (10 mL) and heated in water bath at 50 °C for 5 h. The water layer was extracted with ether (2×10 mL, then with dichlorometane (3×20 mL. The combined dichlorometane extracts were washed with brine, dried over sodium sulfate and evaporated in vacuo to give a colorless oil of 13 (0.82 g, 88 %).

$^1$H-NMR (DMSO-d6, 600 MHz): δ=1.91 (3H), 2.87 (2H, d, *J*=4.65), 3.75 (3H,s), 4.94 (1H, t, *J*=4.65).

$^{13}$C-NMR: 38.7 (3-$CH_2$), 47.9 ($OCH_3$),: 57.6 (2-CH), (169.8 $CH_3$C=O),174.2 (4-C=O), 177.7 (1-C=O).

MW = 188,18 ESI-MS m/z: 188,18 M + H]$^+$ Anal. Calc. for $C_7H_{12}N_2O_4$ C = 44.68 % H=6.43 % *N*=14.89 %. Found C = 44.84 % H = 6.47 % *N*=14.71 %.

The combined ether extracts were washed with 5 % sodium carbonate solution (2×5 mL and brine (10 mL), dried over sodium sulfate and evaporated in vacuo. The solid residue was crystallised from ether-hexane to give ethyl (2-methyl-5-hydroxy-imidazol-4-yl)-acetate (**14**) as white crystals (0.1 g, 12 %).

$^1$H-NMR (DMSO-d6, 600 MHz): δ=3.60 (1, 3H), 8.36 (4, 1H), 2.79 (5, 2H, d, *J*=4.647), 4.82 (11, 1H, t, *J*=4.647).

$^{13}$C-NMR: 22,3 ($CH_3$), 37.8 ($CH_2$), 60.10 ($OCH_2$) 131.4 (Im-4), 156.5 (Im-2), 170.1(CO), 172.4 (Im-5).

MW = 156,14 ESI-MS m/z: 156,15 M + H]$^+$ Anal. Calc. for $C_6H_8N_2O_3$ C = 46.15 % H = 5.16 % *N*=17.94 %.

Found C = 46.23 % H = 5.18 % *N*=17.81 %.

## Computational methods

Starting and resulting structures were drawn and visualized by SYBYL 7.0 [22]. The computations were performed by means of Gaussian 03 software [23]. The conformational search for methyl maleamate was carried out at the B3LYP/6-31+G(d) level in the gas phase [24–26]. In addition to the more standard 6-31G(d) basis set, diffuse functions on heavy atoms were applied in order to get a better representation of the lone pairs involved in hydrogen bonds and also n–π* interactions. The relevant structures were re-optimized in methanol at the IEF-PCM/B3LYP/6-31+G(d)

level [27]. Molecular orbital and charge distribution computations were performed at both levels. Charges were derived by natural population analysis (NPA) [28] as well as by the electrostatic potential using the Merz-Kollman-Sing [29] and CHELPG [30] methods. Molecular orbitals were analyzed and visualized using Gabedit software [31]. In vacuo geometry optimizations and single point calculations were also performed.

The major in-methanol conformers of the adduct were optimized at the IEF-PCM/B3LYP/6-31+G(d) level from approximate geometries. Energy minima were identified by all positive vibrational frequencies. The single point energies were calculated at the IEF-PCM/B3LYP/6-311++G(2df,2pd) level, and thermal corrections were obtained from the IEF-PCM/B3LYP/6-31+G(d) frequency calculations. The relative free energy in the gas phase was calculated as

$$\Delta G(\mathrm{tot,gas}) = \Delta E(\mathrm{gas}) + \Delta G(298,\mathrm{gas}) \quad (1)$$

where ΔE(gas) is the electronic energy in the gas phase, and ΔG(298,gas) is the thermal correction for the free energy in vacuo, at T = 298 K and $p$=1 atm, calculated in the rigid-rotor, harmonic oscillator approximation.

For the in-solution structural isomers,

$$\Delta G(\mathrm{tot,sol}) = \Delta < \Psi|H|\Psi > + \Delta < \Psi|1/2V|\Psi > + \Delta G(\mathrm{drc}) + \Delta G(298,\mathrm{sol}) \quad (2)$$

where H and V stand for the Hamiltonian and the reaction field operator, respectively. Δ<Ψ|H|Ψ> = ΔE(int) and Δ<Ψ|H+1/2V|Ψ> = ΔE(tot) provide the change of the internal energy and the total relative electrostatic free energy of the solutes, respectively. ΔG(drc) stands for the relative dispersion-repulsion-cavity formation free energy, and the definition of ΔG(298,sol) is the same as in Eq. (1), but calculated in solution.

The model follows the conjugate addition of ammonia separately to the vinylogous carbons of the ester or the amide group, forming asparaginate (**a**) or isoasparaginate (**i**) on thermodynamic basis.

The Boltzmann distribution for the product conformers was calculated according to Eq. (3)

$$species\ \% = 100\frac{g_i \exp\left(-\Delta G(\mathrm{tot,sol})_i/k_B T\right)}{\sum_i g_i \exp\left(-\Delta G(\mathrm{tot,sol})_i/k_B T\right)} \quad (3)$$

where $g_i$ is the degeneracy (the number of occurrences of the same energy level) of the species, $\Delta G(\mathrm{tot,sol})_i$ is the total free energy for each species in solution, $k_B$ is the Boltzmann constant, and T is the temperature.

B3LYP/6-31G(d) computations have been used to study cyclization, deamidation and hydrolysis reactions of asparagine moieties in peptides and enzymes [32, 33]. Related reaction mechanisms occur at the ammonia addition to acrolein, acrylonitrile, and acrylic acid [34], at the nucleophilic substitution of 4H-pyran-4-one and 2-methyl-4H-pyran-4-one with ammonia [35]. Calculations of global and local electrophilicity indices were performed for several substituted Michael acceptors [36]. Many of them apply hybrid DFT, especially B3LYP methods. So far, however, no theoretical calculation was reported on the regioselective formation of asparaginates that could predict the ratio of isomers. Chemical reactions of interacting species may lead to different products in the gas phase and in solution [37]. In the case of methyl maleamate we have also taken into account the influence of the interactions of the two carbonyl moieties. On the basis of a literature survey, the B3LYP method was selected for modeling of ammonia addition to methyl maleamate, to predict the addition site and quantitative product ratio.

## Results and discussion

### Synthesis

The Michael reaction is one of the most versatile reactions in organic synthesis owing to its mild reaction conditions, minimal by-product formation, high functional group tolerance and high conversion under optimal conditions [38]. Extensive use of the aza-Michael reaction for the synthesis of alpha- and beta-amino acids led to development of numerous improved methodologies (catalytic [39], chiral catalytic [40, 41], biocatalytic [42], microwave induced [43] procedures).

Efficient control of selectivity during chemical transformations has been of great interest in the field of organic chemistry. Maleamic esters are used as active C4 building blocks due to the presence of two carboxyl groups that enhance the reactivity of the carbon–carbon double bond. Different derivatization of the two carboxyl groups, however, incurs the problem of regioselectivity, since the steric

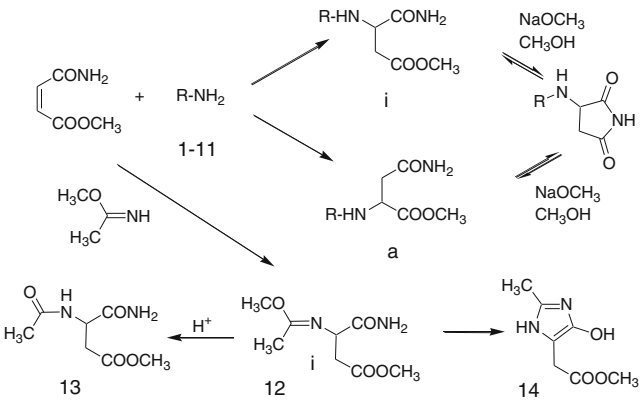


**Fig. 3** 1,4-addition of *N*-nucleophiles to methyl maleamate

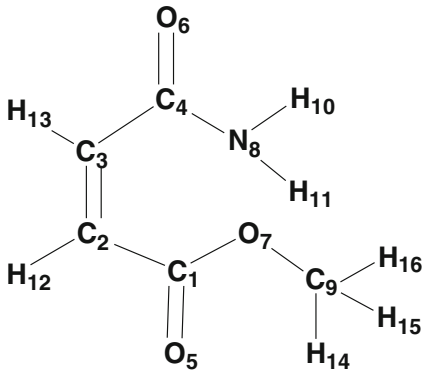


**Fig. 4** Numbering scheme of methyl maleamate

and/or electronic differences of the substituents are usually insufficient to provide control in practical syntheses. To the best of our knowledge, there have been only two reports on this issue, in which a mixture of two regioisomer esters were formed with poor regioselectivity [44, 45]. No data are available in the literature on the addition of ammonia or other amines to unsymmetrical fumaramates or maleamates.

Since amines are both nucleophiles and bases, an additional base catalyst is unnecessary in the investigated additions. Under aza-Michael addition conditions, the ester group in the amide ester acts as a much stronger activating group than the amide so the amine preferentially attacks the β-carbon of the ester group (Fig. 3, Table 1). According to literature reports, ethyl acrylate reacts 85 times faster than acryl amide with nucleophilic agents [46].

Only primary amines were reactive enough to be used for preparation of model compounds. In order to clarify the regioselectivity of the addition we studied the formation of *N*-substituted methyl isoasparaginates and asparaginates in the reaction of different amines (including biogenic amines) bearing various types of subtituents and O-methyl acetimidate with methyl maleamate.

The addition of ammonia and substituted primary amines to methyl maleamate was investigated under identical reaction conditions. Short chain primary aliphatic and aromatic amines were reacted with methyl maleamate leading to the formation of mono-derivatives without additional catalyst at room temperature. Upon increasing the length of the aliphatic group, the reaction rate of the amines with maleamate becomes lower, probably due to the increasing steric hindrance. The formation of methyl asparaginate (**a**) was only found in the case of ammonia, the reaction with any other amine leads exclusively to methyl isoasparaginate (**i**) formation. The steric influence of the *N*-substitutent is a major determining factor in the site of addition. The reactions of methyl maleamate with amines in methanolic solution at room temperature after 24 h provided the *N*-substituted isoasparaginates in medium to good yields (Table 1).

Treatment of *N*-substituted methyl isoasparaginates with sodium methylate in methanol at room temperature led to formation of the appropriate asparaginates as major products via base catalyzed succinimide ring closure and the subsequent ring opening (Table 1).

In addition to these experiments, we investigated the *O*-methyl acetimidate addition for modeling of regioselectivity in methanolic solution under the same conditions, (Fig. 3, Table 1, **13**). After addition, mild acidic hydrolysis provided *N*-acetyl-isoasparagine methylester (**13**) at room temperature. In this reaction, small amounts of side products were formed in a consecutive condensation of the *O*-methyl acetimidate adduct (**12**) by intramolecular ring closure to an imidazole derivative (**14**).

The addition of ammonia led to the formation of both regioisomers. The isomer ratio was found to be 72:28 in methanol at room temperature. We made theoretical calculations, in order to elucidate factors influencing the reactivity and selectivity of addition to the model compound methyl maleamate.

## Modeling and characterization of the conformers of methyl maleamate

### *Geometries and energies*

The title molecule bears rigorous structural constraints. Due to π-electron delocalization over the whole molecular backbone, high stability against rotations around the carbon–carbon single bonds ($C_1$–$C_2$ and $C_3$–$C_4$, Fig. 4) is expected. In the studied C–C=C–C cis isomer, however, considerable repulsion is expected between the oxygens of the end-groups in some arrangements. Such repulsion does not exist in the C–C=C–C trans isomer. Repulsive interactions occur between two carbonyl oxygens, or between the amide carbonyl oxygen and the $sp^3$ oxygen in the ester group. On the other hand, attractive interactions may arise due to an intramolecular hydrogen bond between an amide hydrogen and any oxygen in the ester group. Furthermore, attractive n–π* interactions may come into existence in some non-planar forms, when a carbonyl oxygen lone electron pair is nearly perpendicular to the plane of the other carboxylic function, and the two moieties involved can reach the desired proximity.

In this case, the non-bonding electron pair of the donor group may interact with one of the antibonding orbitals centered mainly on the other carbonyl group [47].

The conformational potential electrostatic surface (PES) was explored in vacuo by rotations in 60° steps around each of the $C_1$–$C_2$ and $C_3$–$C_4$ single bonds in the range (−180°, +180°) for the corresponding torsion angles ($\varphi_{est}$ = $O_7$-$C_1$-$C_2$-$C_3$ and $\varphi_{am}$ = $N_8$-$C_4$-$C_3$-$C_2$; Fig. 4). Based on the low-energy structures obtained, full optimization was performed both in vacuo and in methanol.

**Table 2** Relative energies at different levels of computation and geometric parameters at the B3LYP/6-31+G(d) level for the conformers of methyl maleamate. Energy values are in kcal $mol^{-1}$ units, relative to **m1**. *ΔE(tot)* Total energy in solution, *ΔG(drc)* non-electrostatic solute-solvent interactions (dispersion, repulsion, cavitation), *ΔG(solv)* = ΔE(tot) + ΔG(drc), *ΔE(gas)* total energy in gas phase, *ΔG(298)* relative free energy correction at *T* = 298. *ΔG(tot)* = ΔG(solv) + ΔG(298) in solution and ΔG(tot) = ΔE(gas) + ΔG(298) for the gas phase, respectively

| | IEF-PCM/B3LYP/6-31+G(d) | | | | IEF-PCM/B3LYP/6-311++G(2df,2pd)//IEF-PCM/B3LYP/6-31+G(d) | | | |
|---|---|---|---|---|---|---|---|---|
| | ΔE (tot) | ΔG (solv) | ΔG (298) | ΔG (tot) | ΔE (tot) | ΔG (solv) | ΔG (298) | ΔG (tot) |
| m1 | 0.000 | 0.000 | 0.000 | 0.000 | 0.000 | 0.000 | 0.000 | 0.000 |
| m2 | 3.176 | 3.476 | −0.912 | 2.563 | 3.394 | 3.694 | −0.912 | 2.782 |
| m3 | 1.650 | 2.630 | −1.450 | 1.181 | 1.293 | 2.273 | −1.450 | 0.823 |
| m4 | 2.130 | 2.990 | −1.259 | 1.730 | 1.693 | 2.553 | −1.259 | 1.294 |
| | B3LYP/6-31+G(d) in vacuo | | | | B3LYP/6-311++G(2df,2pd)//B3LYP/6-31+G(d) in vacuo | | | |
| | ΔE (gas) | ΔG (298) | ΔG (tot) | | ΔE (gas) | ΔG (298) | ΔG (tot) | |
| m1 | 0.000 | 0.000 | 0.000 | | 0.000 | 0.000 | 0.000 | |
| m2 | 4.753 | −1.943 | 2.809 | | 4.920 | −1.943 | 2.976 | |
| m3 | n/a | n/a | n/a | | n/a | n/a | n/a | |
| m4 | 5.788 | −1.479 | 4.309 | | 5.087 | −1.479 | 3.608 | |
| Parameter | m1 in vacuo | m1 in methanol | m2 in vacuo | m2 in methanol | m3 in methanol | m4 in vacuo | m4 in methanol | |
| $d(C_3\text{-}C_2)$ | 1.348 | 1.348 | 1.349 | 1.349 | 1.341 | 1.338 | 1.338 | |
| $d(C_3\text{-}C_4)$ | 1.508 | 1.503 | 1.507 | 1.504 | 1.506 | 1.493 | 1.492 | |
| $d(C_2\text{-}C_1)$ | 1.482 | 1.484 | 1.486 | 1.487 | 1.483 | 1.501 | 1.499 | |
| $d(C_4\text{-}O_6)$ | 1.233 | 1.246 | 1.232 | 1.245 | 1.239 | 1.227 | 1.241 | |
| $d(C_1\text{-}O_5)$ | 1.223 | 1.228 | 1.216 | 1.223 | 1.223 | 1.214 | 1.221 | |
| $d(C_3\text{-}H_{13})$ | 1.087 | 1.087 | 1.088 | 1.087 | 1.089 | 1.089 | 1.087 | |
| $d(C_2\text{-}H_{12})$ | 1.087 | 1.086 | 1.087 | 1.087 | 1.086 | 1.088 | 1.088 | |
| $d(C_1\text{-}O_7)$ | 1.347 | 1.339 | 1.358 | 1.343 | 1.345 | 1.341 | 1.336 | |
| $d(C_4\text{-}N_8)$ | 1.353 | 1.344 | 1.355 | 1.344 | 1.346 | 1.37 | 1.353 | |
| $d(N_8\text{-}H_{10})$ | 1.011 | 1.013 | 1.012 | 1.013 | 1.012 | 1.01 | 1.011 | |
| $d(N_8\text{-}H_{11})$ | 1.018 | 1.020 | 1.011 | 1.013 | 1.014 | 1.011 | 1.013 | |
| $d(O_7\text{-}C_9)$ | 1.441 | 1.448 | 1.446 | 1.452 | 1.446 | 1.442 | 1.450 | |
| $a(C_3\text{-}C_2\text{-}H_{13})$ | 115.87 | 115.51 | 114.99 | 114.76 | 118.68 | 118.98 | 119.07 | |
| $a(C_3\text{-}C_2\text{-}C_4)$ | 135.34 | 134.84 | 137.12 | 136.41 | 127.67 | 123.07 | 123.03 | |
| $a(C_2\text{-}C_3\text{-}H_{10})$ | 116.99 | 116.53 | 115.89 | 115.62 | 119.67 | 119.56 | 119.67 | |
| $a(C_2\text{-}C_3\text{-}C_1)$ | 130.23 | 130.60 | 135.42 | 134.90 | 124.26 | 126.05 | 126.29 | |
| $a(C_4\text{-}C_3\text{-}N_8)$ | 119.57 | 119.98 | 120.27 | 120.71 | 116.68 | 114.73 | 115.11 | |
| $a(C_4\text{-}C_3\text{-}O_6)$ | 117.13 | 117.24 | 117.14 | 116.94 | 119.47 | 123.10 | 122.23 | |
| $a(C_1\text{-}C_2\text{-}O_7)$ | 109.69 | 109.79 | 116.68 | 116.61 | 110.63 | 112.35 | 112.39 | |
| $a(C_1\text{-}C_2\text{-}O_5)$ | 128.11 | 127.60 | 121.33 | 120.79 | 125.78 | 122.44 | 122.93 | |
| $a(O_7\text{-}C_1\text{-}C_9)$ | 116.31 | 117.03 | 115.75 | 116.94 | 116.78 | 115.72 | 116.70 | |
| HB length[a] | 1.834 | 1.819 | 1.875 | 1.876 | n/a | n/a | n/a | |
| Φest $O_7\text{-}C_1\text{-}C_2\text{-}C_3$ | 180 | 179.61 | 0.01 | 8.95 | 176.11 | −78.34 | −87.03 | |
| Φam $N_8\text{-}C_4\text{-}C_3\text{-}C_2$ | 0.01 | −0.12 | 0.04 | −13.22 | −83.48 | 173.762 | 176.31 | |

[a] HB lengths refer to the corresponding O···H distances

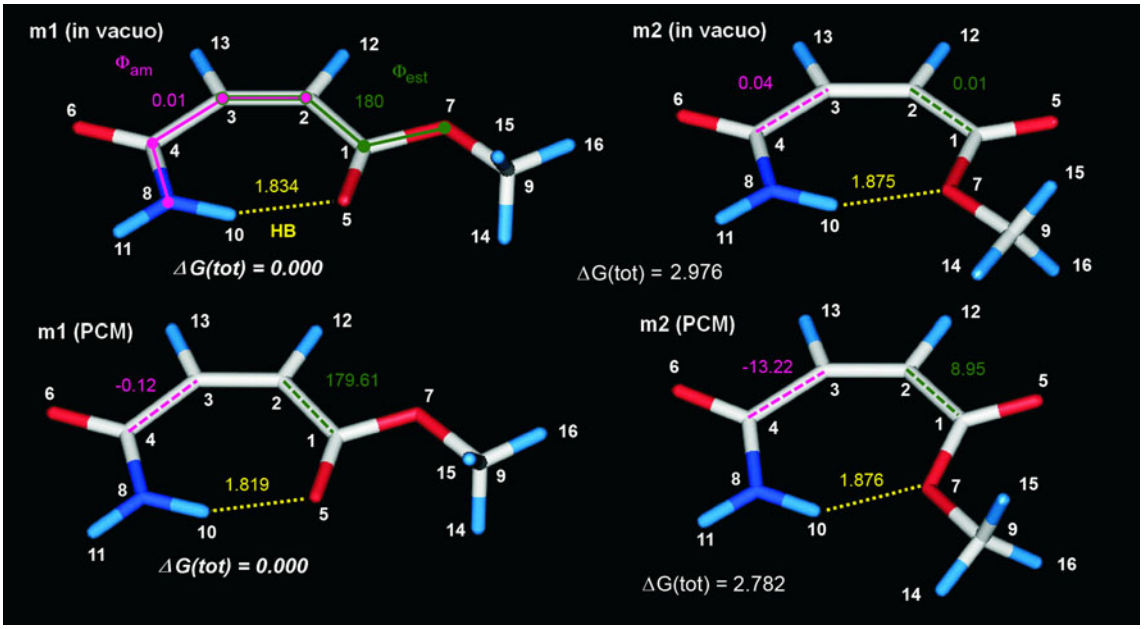


**Fig. 5** Structures of **m1** and **m2** stabilized by hydrogen bridges in vacuo and in methanol. *Purple numbers* Dihedral angles defined by atoms $N_8$-$C_4$-$C_3$-$C_2$ (Φam), *green numbers* $O_7$-$C_1$-$C_2$-$C_3$ dihedral angles (Φest); all values in degrees. *Yellow numbers* Length of intramolecular hydrogen bonds (Ångstroms). A more detailed geometric comparison is given in Table 2

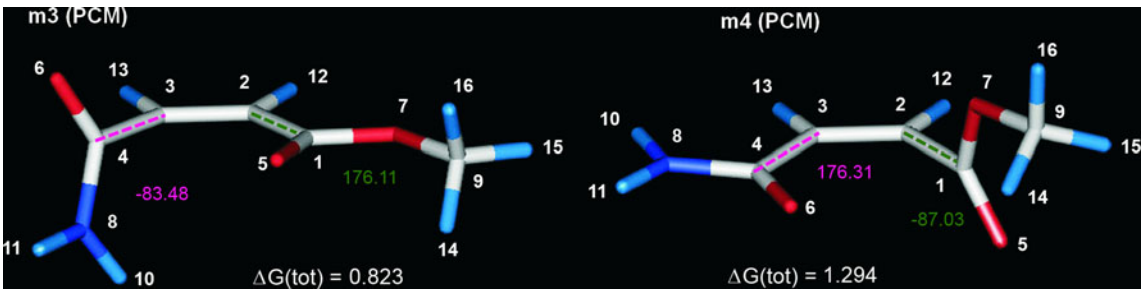


**Fig. 6** Structures of **m3** and **m4** with n–π* interactions in methanol (see legend to Fig. 5 for details, full geometric details in Table 2)

Two, primarily planar minima were found both in vacuo and in methanol. The deepest minimum was found for **m1** with $\varphi_{am} \approx 0°$ and $\varphi_{est} \approx 180°$. For **m2** in methanol, the torsion angles deviate by about 10°. (See Table 2).

**Table 3** Molecular orbital (MO) coefficients for the three highest occupied MOs (HOMO) in **m3** and **m4** conformers of methyl maleamate

| m3 | | | | m4 | | | |
|---|---|---|---|---|---|---|---|
| $O_5$ | HOMO-2 | HOMO-1 | HOMO | $O_6$ | HOMO-2 | HOMO-1 | HOMO |
| IEF-PCM/B3LYP/6-31+G(d) | | | | | | | |
| $2p_x$ | 0.49 | 0.18 | −0.07 | $2p_x$ | 0.07 | −0.09 | 0.43 |
| $2p_y$ | 0.17 | 0.04 | −0.01 | $2p_y$ | 0.17 | 0.05 | −0.39 |
| $2p_z$ | −0.07 | 0.04 | −0.10 | $2p_z$ | 0.40 | −0.04 | 0.06 |
| IEF-PCM/B3LYP/6-311++G(2df,2pd) | | | | | | | |
| $2p_x$ | 0.23 | 0.09 | −0.03 | $2p_x$ | 0.04 | 0.04 | 0.20 |
| $2p_y$ | 0.08 | 0.02 | −0.01 | $2p_y$ | 0.08 | −0.03 | −0.18 |
| $2p_z$ | −0.03 | 0.02 | −0.04 | $2p_z$ | 0.19 | 0.00 | 0.03 |

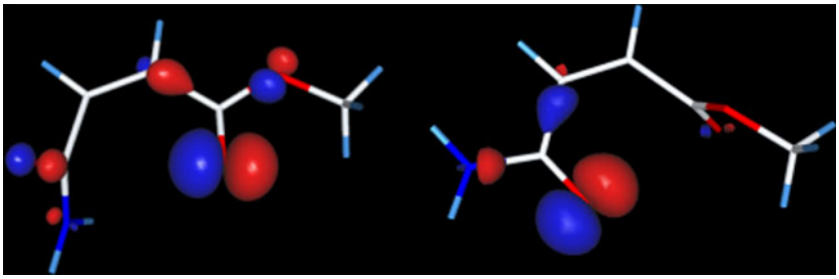

**Fig. 7** Highest occupied molecular orbital (HOMO)-2 orbital for **m3** (left) and HOMO for **m4** (right) (with 6-311++G (2df,2pd) basis set)

The stability of these structures is due primarily to their nearly co-planar heavy atom skeletons and an intramolecular N–H···O hydrogen bond (Fig. 5).

The conformer **m1** is still lower in ΔE(tot) by as much as almost 5 kcal mol$^{-1}$ in vacuo and by about 3.4 kcal mol$^{-1}$ in methanol. The N–H···O = C hydrogen bonds are, however, shorter than the ones between the amide N–H and the sp$^3$ ester oxygen (Table 2). This considerable energy difference can be interpreted as the consequence of a more expressed hydrogen-bond acceptor character for a carbonyl than that of an sp$^3$ oxygen. As a result, the ΔG(298) correction is about −1 to −2 kcal mol$^{-1}$ (Table 2). The population of **m1** is still overwhelming both in the gas phase and in methanol.

Independently of the PES scan, we also sought for conformers stabilized by n–π* interactions. Due to symmetry, three types of such methyl maleamate conformers may exist. One of the carbonyl oxygens, or the sp$^3$ oxygen of the ester group can donate a lone electron pair to the carbonyl carbon of the other carboxyl-derivative group. The two conformers with the carbonyl oxygen donors (referred as **m3** and **m4**), were found in methanol (Fig. 6) [47], but only **m4** was found in vacuo.

It is thought that the proximity of the amide hydrogen and the sp$^2$ ester oxygen leads to the destabilization of **m3** and to the conversion of **m1**.

Conformer **m4** is of high free energy (3.6–4.3 kcal mol$^{-1}$) and it barely appears in the equilibrium mixture. Methanol, however, largely stabilizes conformers **m3** and **m4** providing a relative G(tot) of 1–2 kcal mol$^{-1}$ (Table 2). Thus occurrence of these conformers is allowed, albeit in low populations.

### *Comparative analysis of the molecular orbitals of the conformers*

Molecular orbital calculations were performed to interpret the results for conformers **m3** and **m4**. The n–π* interactions may be encountered if high LCAO-MO coefficients for atomic orbitals of one of the oxygens are found in HOMO, HOMO-1 or HOMO-2, and the directions of these atomic orbitals permit the interaction with other orbitals at a nearby amide/ester carbon atom. According to the literature data, for characterizing regioselectivity of the thiolate addition to unsymmetrical fumarate esters, coefficients of LUMO were

**Table 4** Charges calculated with different methods in vacuo and in solvent environment for the conformers of the methyl maleamate

| | m1 | | m2 | | m3 | | m4 | |
|---|---|---|---|---|---|---|---|---|
| | $C_3$ | $C_2$ | $C_3$ | $C_2$ | $C_3$ | $C_2$ | $C_3$ | $C_2$ |
| IEF-PCM/B3LYP/6-31+G(d) | | | | | | | | |
| NPA | −0.22 | −0.29 | −0.23 | −0.29 | −0.22 | −0.32 | −0.30 | −0.24 |
| CHELPG | −0.15 | −0.31 | −0.18 | −0.30 | −0.15 | −0.35 | −0.18 | −0.38 |
| MKS | −0.16 | −0.43 | −0.19 | −0.40 | −0.24 | −0.42 | −0.12 | −0.57 |
| B3LYP/6-31+G(d) in vacuo | | | | | | | | |
| NPA | −0.20 | −0.32 | −0.22 | −0.31 | n/a | n/a | −0.31 | −0.22 |
| CHELPG | −0.11 | −0.34 | −0.16 | −0.30 | n/a | n/a | −0.18 | −0.33 |
| MKS | −0.12 | −0.45 | −0.19 | −0.38 | n/a | n/a | −0.13 | −0.50 |
| IEF-PCM/B3LYP/6-311++G(2df,2pd) | | | | | | | | |
| NPA | −0.18 | −0.26 | −0.19 | −0.25 | −0.18 | −0.29 | −0.26 | −0.20 |
| CHELPG | −0.15 | −0.29 | −0.17 | −0.29 | −0.15 | −0.33 | −0.17 | −0.37 |
| MKS | −0.15 | −0.41 | −0.18 | −0.39 | −0.23 | −0.41 | −0.12 | −0.55 |
| B3LYP/6-311++G(2df,2pd) in vacuo | | | | | | | | |
| NPA | −0.16 | −0.28 | −0.18 | −0.27 | n/a | n/a | −0.27 | −0.18 |
| CHELPG | −0.11 | −0.31 | −0.16 | −0.28 | n/a | n/a | −0.18 | −0.31 |
| MKS | −0.12 | −0.43 | −0.18 | −0.36 | n/a | n/a | −0.13 | −0.48 |

**Table 5** Electronic energies, solvation energies, thermodynamic quantities and the distinctive structural properties of the adduct conformers. Energies in kcal $mol^{-1}$ relative to ***i1***. For term definitions, see Table 2. HB lengths refer to the corresponding O···H or N···H distances, and are in Ångstroms

| | ΔE(int) | ΔE(tot) | ΔG(drc) | ΔG(solv) | ΔG(298) | ΔG(tot) |
|---|---|---|---|---|---|---|
| i1 | 0.000 | 0.000 | 0.000 | 0.000 | 0.000 | 0.000 |
| i2 | 0.082 | 0.694 | −0.160 | 0.534 | −0.138 | 0.396 |
| i3 | 3.109 | 1.367 | 0.080 | 1.447 | −0.004 | 1.444 |
| i4 | 3.409 | 1.261 | 0.270 | 1.531 | 0.247 | 1.778 |
| i5 | 4.251 | 1.654 | 0.380 | 2.034 | −0.206 | 1.828 |
| i6 | 2.362 | 2.525 | −0.520 | 2.005 | −0.023 | 1.983 |
| i7 | 4.412 | 1.812 | 0.460 | 2.272 | 0.252 | 2.523 |
| a1 | 4.041 | 0.863 | 0.440 | 1.303 | −0.658 | 0.645 |
| a2 | 3.453 | 1.516 | 0.230 | 1.746 | −0.905 | 0.841 |
| a3 | 3.477 | 1.752 | 0.610 | 2.362 | −0.946 | 1.416 |
| a4 | 6.045 | 2.356 | 0.680 | 3.036 | −1.517 | 1.520 |
| a5 | 6.626 | 1.915 | 0.520 | 2.435 | −0.854 | 1.581 |
| a6 | 2.802 | 1.943 | 0.160 | 2.103 | −0.436 | 1.667 |
| a7 | 2.670 | 1.383 | 0.090 | 1.473 | 0.629 | 2.102 |
| a8 | 8.272 | 3.289 | 0.710 | 3.999 | −0.747 | 3.252 |
| | $C_1$-$C_2$-$C_3$-$C_4$ | $C_1$-$C_2$-$C_3$-$N_{17}$ | HB donor | HB acceptor | HB length | |
| i1 | −65.7 | 63.2 | amide(I), amine(II) | amine(I), ester $Osp^2$(II) | 2.222(I), 2.395(II) | |
| i2 | 168.7 | −69.1 | amide(I), amine(II) | amine(I), ester $Osp^2$(II) | 2.232(I), 2.208(II) | |
| i3 | 164.4 | −73.5 | amide(I), amine(II) | amine(I), ester $Osp^3$(II) | 2.234(I), 2.268(II) | |
| i4 | −54.6 | 74.5 | amide(I), amine(II) | amine(I), ester $Osp^3$(II) | 2.247(I), 2.322(II) | |
| i5 | 68.9 | −169.7 | amide | amine | 2.249 | |
| i6 | 85.0 | −154.4 | amide(I), amine(II) | ester O $sp^2$(I), amide $Osp^2$(II) | 1.946(I), 2.254(II) | |
| i7 | −70.7 | 54.0 | amide | amine | 2.234 | |
| a1 | 167.0 | −67.6 | amine | ester $Osp^2$ | 2.610 | |
| a2 | −61.6 | 67.4 | amine(I,II) | amide $Osp^2$(I), ester $Osp^2$(II) | 2.426(I), 2.671(II) | |
| a3 | 62.1 | −175.1 | none | none | none | |
| a4 | 57.9 | −177.7 | none | none | none | |
| a5 | 165.3 | −67.4 | amine | ester $Osp^3$ | 2.523 | |
| a6 | −64.5 | 66.5 | amine(I,II) | amide $Osp^2$(I), ester $Osp^3$(II) | 2.384(I), 2.549(II) | |
| a7 | −57.7 | 65.6 | amide(I), amine(II) | amine(I), ester $Osp^2$(II) | 2.046(I), 2.393(II) | |
| a8 | 70 | −162.5 | amine | ester $Osp^3$ | 2.495 | |

calculated by the PM3 semiempirical method [45]. Due to the trans-orientation in fumarates, there are no direct interactions between the two carboxyl moieties, which makes their modeling simpler than that of the maleate derivatives. The selected coefficients in Table 3 indicate that the HOMO-2 for **m3** and the HOMO for **m4** nearly correspond to lone pairs of an $sp^2$ oxygen.

By drawing the electron density surface for these orbitals (Fig. 7), the orientations of the lobes allow the oxygens acting as donor atoms for n–π* interactions. These orbitals are mainly built of the $p_x$ and $p_y$ orbitals of the two $sp^2$ oxygens.

The symmetry axes of the corresponding lone pairs on the oxygens lie in the line connecting the oxygen and the carbonyl carbon in the other group. Results obtained with the 6-31+G(d) basis set agree with those from 6-311++G(2df,2pd) basis set calculations.

*Charge distributions of the conformers*

Charge distributions calculated with two different basis sets in the gas phase and in methanol are compared in Table 4 for selected charges. The aim of the calculations was to see whether the charge distribution of the isolated methyl maleamate can predict the site of the nucleophilic attack.

The less negative charge is favorable in this respect. In terms of negativity, the relation $C_2 > C_3$ holds with all three methods for conformers **m1**, **m2** and **m3**. Only the natural population analysis (NPA) method predicts slightly more negative charge for $C_3$ in **m4**, but this conformer is a minor component in the equilibrium mixture.

Thus the results for the major reaction site are in accord with the experiments regarding the amine additions. Since the charge difference is present both in gas phase and in

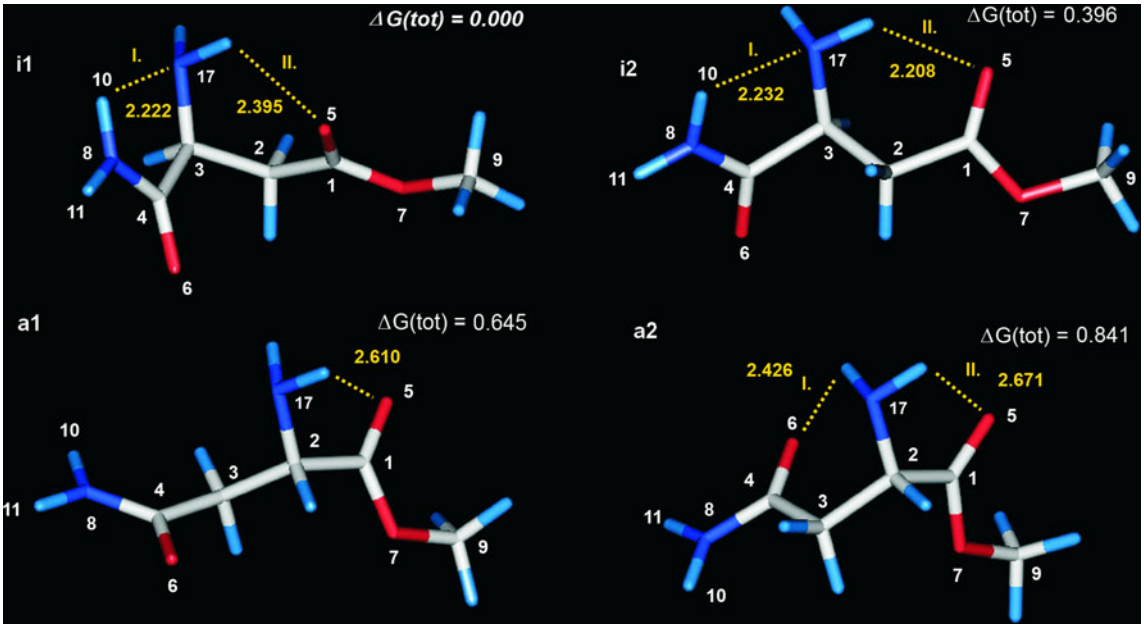


**Fig. 8** The most stable product conformers: **i1**, **i2**, **a1** and **a2**. *Yellow numbers* Lengths of hydrogen bonds

methanol, the less negative $C_3$ compared to $C_2$ atom is apparently an intrinsic property of the structures.

## Reaction product calculations for the Michael addition with ammonia

Experimental analysis of the reaction products indicated the preference of the 1,4 amine additions to methyl maleamate. Concerning calculations, it is difficult to reach local minima and/or TS structures for clusters of molecules, and convergence problems are also likely with larger basis sets. Furthermore, many of the reached local minima for these van der Waals complexes may be of little interest for the reaction PES. Thus the question remained whether the theory could predict energetically the preference of the experimentally observed isoasparaginate product. For the reaction products, geometries of three major staggered conformations with $C_1$-$C_2$-$C_3$-$C_4$ dihedral angles of approximately ±60° (gauche$^+$, gauche$^-$) and 180° (trans) were optimized for each of the isoasparaginate and asparaginate adducts in methanol. However, because of the possibility of intramolecular hydrogen-bonds between the amine, amide and the ester groups, consideration of further conformers in accord with the conformations above became important. A total of seven isoasparaginate and eight asparaginate conformers were found (Table 5). As of lowest total energy and free energy, an isoasparaginate structure, **i1**, was found in accord with the experiment. This structure corresponds to a $C_1$-$C_2$-$C_3$-$C_4$ gauche$^-$ species with two intramolecular bonds.

All energy data in Table 5 are relative values referring to the corresponding **i1** term. The basically trans **i2** conformer is of higher free energy by only 0.40 kcal mol$^{-1}$. Both **i1** and **i2** are stabilized by two intramolecular hydrogen bonds. Two low free-energy asparaginate isomers, **a1** and **a2** were identified with relative ΔG(tot) values of 0.64 and 0.84 kcal mol$^{-1}$, respectively. Structures corresponding to the two isoasparaginate and asparaginate conformers with the lowest ΔG(tot) values are shown in Fig. 8.

The overall ratio for the isoasparaginate and asparaginate products coming from Eq. (3) is about 67:33, provided the system is in thermodynamic equilibrium. The weak internal H-bonds play a crucial role in stabilizing the lowest energy conformers.

All of the isomers/conformers (Table 5) other than the abovementioned four have relative free energies of more than 1.4 kcal mol$^{-1}$ in contrast to **i1**, thus their populations in the equilibrium mixture are minor at T = 298 K.

## Conclusions

Maleate and fumarate—two isomeric unsaturated dicarboxylic acids—are products of different metabolic processes and play important biological roles in living organisms including formation of aspartate derivatives. The reactivity of methyl maleamate toward different types of primary amines in regioselective asparagine formation was studied to provide insight into the mechanism of aspartyl-isoaspartyl formation. An *N*-substituted series of asparaginate and isoasparaginate derivatives was synthesized to examine the influence of electronic and steric constraints of maleamate and nucleophilicity of the amine substituents. Regioselectivity was characterized by determination of isomer ratio in the aza-Michael addition

and the base-catalyzed equilibrium between the isomers in methanol solution.

In the reactions of substituted amines and maleamate a regioselective process provided only the N-substituted-isoasparagines. Both isomers were formed in reaction of maleamate with ammonia.

Theoretical calculations at the B3LYP/6-311++G(2df,2pd)//B3LYP/6-31+G(d) level were performed to elucidate the influencing factors of regioselectivity. Methyl maleamate conformers were studied in vacuo and in methanol (IEF-PCM approach). Calculated charge distributions predict that a nucleophilic attack at the C = C double bond is more favorable at the C atom adjacent the amide rather than the ester group. The addition products were also characterized theoretically by calculating relative free energies in methanol. The results predict the thermodynamically favorable formation of methyl isoasparaginate, the calculated ratio for the isoasparaginate and asparaginate adducts is about 2 : 1 in the equilibrium mixture, in good agreement with experimental results.

## References


1. Clarke S, Stephenson RC, Lowenson JD (1992) Chemical and physical pathways of protein degradation. Stability of protein pharmaceuticals Pt. A. Plenum, New York, pp 1–29
2. Manning MC, Chou DK, Murphy BM, Payne RW, Katayama DS (2010) Stability of protein pharmaceuticals: an update. Pharm Res 27(4):544–575
3. Clarke S (1987) Propensity for spontaneous succinimide formation from aspartyl and asparaginyl residues in cellular proteins. Int J Pept Protein Res 30:808–821
4. Aswad DW (1995) Deamidation and isoaspartate formation in peptides and proteins. CRC, Boca Raton
5. Husbyn M, Ørning L, Cuthbertson A, Fischer PM (1999) Linear analogues derived from the first EGF-like domain of human blood coagulation factor VII: enhanced inhibition of FVIIa/TF complex activity by backbone modification through aspartimide formation. J Pept Sci 5:323–329
6. Radkiewicz JL, Zipse H, Clarke S, Houk KN (1996) Accelerated racemization of aspartic acid and asparagine residues via succinimide intermediates: an ab initio theoretical exploration of mechanism. J Am Chem Soc 118:9148–9155
7. Clarke S (2003) Aging as war between chemical and biochemical processes: protein methylation and the recognition of age-damaged proteins for repair. Ageing Res Rev 2:263–285
8. Šoškić V, Groebe K, Schrattenholz A (2008) Nonenzymatic post-translational protein modifications in ageing. Exp Gerontol 43:247–257
9. Johnson BA, Murray ED Jr, Clarke S, Glass DB, Aswad DW (1987) Protein carboxyl methyltransferase facilitates conversion of atypical L-isoaspartyl peptides to normal L-aspartyl peptides. J Biol Chem 262:5622–5629
10. Athmer L, Kindrachuk J, Georges F, Napper S (2002) The influence of protein structure on the products emerging from succinimide hydrolysis. J Biol Chem 277:30502–30507
11. Puthan Veetil V, Raj H, Quax WJ, Janssen DB, Poelarends GJ (2009) Site-directed mutagenesis, kinetic and inhibition studies of aspartate ammonia lyase from *Bacillus* sp. YM55-1. FEBS J 276:2994–3007
12. Breuer M, Ditrich K, Habicher T, Hauer B, Keßeler M, Stürmer R, Zelinski T (2004) Industrial methods for the production of optically active intermediates. Angew Chem Int Ed 43:788–824
13. Weiner B, Poelarends GJ, Janssen DB, Feringa BL (2008) Biocatalytic enantioselective synthesis of N-substituted aspartic acids by aspartate ammonia lyase. Chem Eur J 14:10094–10100
14. Jin JH, Choi KK, Jung US, In YH, Lee SY, Lee J (2004) Regulatory analysis of amino acid synthesis pathway in Escherichia coli: aspartate family. Enzyme Microb Technol 35:694–706
15. Cain RB, Houghton C, Wright KA (1974) Microbial metabolism of the pyridine ring. Biochem J 140:293–300
16. Jimenez JI, Canales A, Jimenez-Barbero J, Ginalski K, Rychlewski L, Garcıa JL, Dıaz E (2008) Deciphering the genetic determinants for aerobic nicotinic acid degradation: the nic cluster from Pseudomonas putida KT2440. Proc Natl Acad Sci USA 105(32):11329–11334
17. Van der Werf MJ, Van den Tweel WJJ, Hartmans S (1992) Screening for microorganisms producing D-malate from maleate. Appl Environ Microbiol 58:2854–2860
18. Hanson KR, Havir EA (1972) The enzymic elimination of ammonia. In: Boyer PD (ed) The enzymes, vol 3. Academic, New York, pp 75–166
19. Boros M, Kökösi J, Vámos J, Kövesdi I, Noszál B (2007) Methods for syntheses of N-methyl-DL-aspartic acid derivatives. Amino Acids 33:709–717
20. Boros M, Kökösi J, Vámos J, Noszál B (2007) Complete resolution of the microscopic protonation equilibria of N-methyl-D-aspartic acid and related compounds. J Pharm Biomed Anal 43:1306–1314
21. DeHart MP, Anderson BD (2007) The role of the cyclic imide in alternate degradation pathways for asparagine-containing peptides and proteins. J Pharm Sci 96:2667–2685
22. SYBYL® 7.0, Tripos, St. Louis, MO
23. Frisch MJ, Trucks GW, Schlegel HB, Scuseria GE, Robb MA (2003) Gaussian 03, Gaussian, Wallingford
24. Hehre WJ, Radom L, Schleyer PR, Pople JA (1986) Ab initio molecular orbital theory. Wiley, New York
25. Lee C, Yang W, Parr RG (1988) Development of the Colle-Salvetti correlation-energy formula into a functional of the electron density. Phys Rev B 37:785–789
26. Becke AD (1993) Density-functional thermochemistry. III. The role of exact exchange. J Chem Phys 98:5648–5652
27. Miertuš S, Scrocco E, Tomasi J (1981) Electrostatic interaction of a solute with a continuum. A direct utilizaion of AB initio molecular potentials for the prevision of solvent effects. Chem Phys 55:117–129
28. Carpenter JE, Weinhold F (1988) Analysis of the geometry of the hydroxymethyl radical by the "different hybrids for different spins" natural bond orbital procedure. J Mol Struct (THEOCHEM) 169:41–62
29. Singh UC, Kollman PA (1984) An approach to computing electrostatic charges for molecules. J Comput Chem 5:129–145
30. Breneman CM, Wiberg KB (1990) Determining atom-centered monopoles from molecular electrostatic potentials. The need for high sampling density in formamide conformational analysis. J Comput Chem 11:361–373
31. Allouche AR (2011) Gabedit—a graphical user interface for computational chemistry softwares. J Comput Chem 32:174–182
32. Konuklar FAS, Aviyente V, Sen TZ, Bahar I (2001) Modeling the deamidation of asparagine residues via succinimide intermediates. J Mol Model 7:147–160
33. Takahashi O, Oda A (2012) Amide–iminol tautomerization of the C-terminal peptide groups of aspartic acid residues: two-water-assisted mechanism, cyclization from the iminol tautomer leading

to the tetrahedral intermediate of succinimide formation, and implication to peptide group hydrogen exchange. In: Jones JE, Moreno DE (eds) Tyrosine and aspartic acid: properties, sources, and health benefits. Nova, Hauppauge, NY, pp 131–147
34. Pardo L, Osman R, Weinstein H, Rabinowitz JR (1993) Mechanisms of nucleophilic addition to activated double bonds: 1,2- and 1,4-Michael addition of ammonia. J Am Chem Soc 115:8263–8269
35. Kóňa J, Zahradník P, Fabian WMF (2003) Ab initio and density functional theory studies on the mechanism of nucleophilic vinylic substitution of 4H-pyran-4-one and 2-methyl-4H-pyran-4-one with ammonia. Theor Chem Accounts 109:176–181
36. Contreras R, Domingo LR, Pérez P (2004) A theoretical study on the regioselectivity of 1,3-dipolar cycloadditions using DFT-based reactivity indexes. Tetrahedron 60:11503–11509
37. Tezer N, Ozkan R (2001) Mechanisms and transition structures for conjugate and carbonyl addition of ammonia to three small α,β-unsaturated carbonyl compounds. An ab initio molecular orbital study. J Mol Struct (THEOCHEM) 546:79–88
38. Gimbert C, Moreno-Mañas M, Pérez E, Vallribera A (2007) Tributylphosphine, excellent organocatalyst for conjugate additions of non-nucleophilic N-containing compounds. Tetrahedron 63:8305–8310
39. Mukherjee C, Misra AK (2007) Aza-Michael addition of amines to activated alkenes catalyzed by silica supported perchloric acid under a solvent-free condition. Lett Org Chem 4:54–59
40. Davies SG, Garrido NM, Kruchinin D, Ichihara O, Kotchie LJ, Price PD, Mortimer AJP, Russell AJ, Smith AD (2006) Homochiral lithium amides for the asymmetric synthesis of β-amino acids. Tetrahedron-Asymmetry 17:1793–1811
41. Bai JF, Wang LL, Peng L, Guo YL, Jia LN, Tian F, He GY, Xu XY, Wang LX (2012) Asymmetric Michael addition of α-substituted isocyanoacetates with maleimides catalyzed by chiral tertiary amine thiourea. J Org Chem 77(6):2947–2953
42. Szymanski W, Wu B, Weiner B, De Wildeman S, Feringa BL, Janssen DB (2009) Phenylalanine aminomutase-catalyzed addition of ammonia to substituted cinnamic acids: a route to enantiopure α- and β-amino acids. J Org Chem 74:9152–9157
43. Escalante J, Carrillo-Morales M, Linzaga I (2008) Michael additions of amines to methyl acrylates promoted by microwave irradiation. Molecules 13:340–347
44. Zaderenko P, López MC, Ballesteros P (1996) Addition of azoles and amines to unsymmetrical fumaric esters. J Org Chem 61:6825–6828
45. Kamimura A, Murakami N, Kawahara F, Yokota K, Omata Y, Matsuura K, Oishi Y, Morita R, Mitsudera H, Suzukawa H, Kakehi A, Shirai M, Okamoto H (2003) On the regioselectivity for the Michael addition of thiols to unsymmetrical fumaric derivatives. Tetrahedron 59:9537–9546
46. Götz MG, James KE, Hansell E, Dvořák J, Seshaadri A, Sojka D, Kopáček P, McKerrow JH, Caffrey CR, Powers JC (2008) Aza-peptidyl Michael acceptors. A new class of potent and selective inhibitors of asparaginyl endopeptidases (legumains) from evolutionarily diverse pathogens. J Med Chem 51:2816–2832
47. Akakura M, Koga N (2002) Theoretical study of dimethyl maleate and its complexes with Lewis acids: effect of the interaction between two methoxycarbonyl groups on equilibrium structures. Bull Chem Soc Jpn 75:1785–1793